



Norwegian University of
Science and Technology

EFFECT OF Ni ADDITIONS ON MECHANICAL PROPERTIES AND MICROSTRUCTURE OF THE A356 ALUMINIUM FOUNDRY ALLOY

Federico Poli

Light Metals Production

Submission date: March 2016

Supervisor: Marisa Di Sabatino, IMTE

Co-supervisor: Daniele Casari, IFY

Li Yanjun, IMT

Norwegian University of Science and Technology
Department of Materials Science and Engineering



NTNU – Trondheim
Norwegian University of
Science and Technology

Department of Materials Science and Engineering
Norwegian University of Science and Technology
Alfred Getz vei 2 B, N-7491 Trondheim, Norway

EFFECT OF Ni ADDITIONS ON MECHANICAL PROPERTIES AND MICROSTRUCTURE OF THE A356 ALUMINIUM FOUNDRY ALLOY

Candidate: Federico Poli

Submission date: March 2015

Supervisor: Prof. Marisa Di Sabatino Lundberg, IMTE

Cosupervisors: Dr. Daniele Casari (IFY) and Prof. Yanjun Li (IMT)

Table of contents

Introduction	7
1.Theoretical background	9
1.1 The A356 aluminium casting alloy and the T6 heat treatment	9
1.2 The influence of Ni	10
2. Materials and Methods	13
2.1 Preparation of the alloys	13
2.1.1 Chemical analysis	14
2.1.2 Thermal analysis	16
2.2 Preparation of the samples	18
2.2.1. Casting and T6 heat treatment	18
2.2.2. Machining of the tensile and Charpy impact samples	19
2.3 High-temperature tensile tests	21
2.4 Charpy impact tests	22
2.5 Microstructural analysis	23
3.Results	25
3.1 Characteristic temperatures	25
3.2 High-temperature mechanical properties	28
3.3 Impact properties	30
3.4 Microstructural investigation	32
4 Discussion	45
Conclusions	47
Acknowledgements	49
Bibliography	51

To my mother

In the end i realized that the only way to stop learning is to
keep discovering

Introduction

Typically, hyper-eutectic Ni-rich Al-Si alloys are used for high-temperature applications. The influence of such alloying element on the mechanical properties of hypo-eutectic Al-Si alloys, however, has not been studied in detail, yet.

In this thesis, the effect of three different Ni additions (0.5, 1 and 2 wt.%) on the mechanical properties and microstructure of the commercial purity unmodified A356 (AlSi7Mg0.3) aluminium foundry alloy was investigated. A tensile testing machine was employed to obtain the stress-strain curves at high temperature of the prepared alloys, and Charpy impact tests were performed to assess the amount of energy absorbed by the material during fracture. Microstructural investigations were carried out by means of Optical Microscopy (OM) and scanning electron microscopy (SEM) in order to identify the main micro-structural phases and the intermetallic compounds precipitated during solidification. Thirty castings were for tensile and Charpy impact tests were obtained by means of permanent mould casting, as well as specimens for the analysis of the chemical composition via glow discharge optical emission spectroscopy (GD-OES) and for thermal analysis. Ten specimens were obtained for each Ni addition, five in the as-cast and five in the T6 heat-treated condition.

Tensile specimens were subjected to high-temperature tensile tests at 235 °C to obtain the stress-strain curves and the values of yield strength ($R_{p0.2}$), ultimate tensile stress (UTS) and percentage elongation (A) were obtained. Further specimens machined from the bottom part of the risers were subjected to Charpy impact tests and the energy absorbed by the material during fracture was measured. Other parameters such crack initiation (W_m) and crack propagation energies (W_p) as well as the maximum load required to break the specimens (F_{max}) were calculated. Also emphasis was given to the effect of the different Ni additions and to the importance of T6 in increasing the mechanical properties of this foundry alloy.

The assumptions on the intermetallic phases that formed during solidification were proven using the post-solidification microstructural observations. The presence of Al_3Ni and Al_9FeNi Ni-rich intermetallic compounds was correlated to the mechanical properties of the alloys.

1. Theoretical background

1.1 The A356 aluminium casting alloy and the T6 heat treatment

The A356 aluminium foundry alloy (Al-7wt% Si-0.3wt% Mg) is one of the most widely used Al-Si alloys in automotive and aerospace industries for critical structure applications due to its good mechanical properties in the heat treated condition and corrosion resistance[1].

However, it is well-known that the yield strength ($R_{p0.2}$) and the ultimate tensile strength (UTS) of such alloy rapidly decrease as temperature increases. Accordingly, it is of particular interest to improve the elevated-temperature properties of the A356 alloy, for example by adding specific alloying elements such as Ni to form some thermally stable rigid intermetallic phases, e.g. the Al_3Ni and the Al_9FeNi phases.

The chemical composition of the A356 alloy (also named EN AB-42100) in accordance with the 1676-2010 specification is given in Table 1.

Si	Mg	Fe	Cu	Mn	Zn	Ti	Others	Al
6.50-7.50	0.30-0.45	<0.15	<0.03	<0.10	<0.07	<0.18	<0.10	Bal.

Table 1-
Chemical composition (wt.%) of the A356 aluminium foundry alloy in accordance with the EN 1676-2010 specification.

The microstructure of the A356 alloy [1] in the as-cast condition generally consists of primary α -Al dendrites and an Al-Si eutectic mixture. Some intermetallic compounds such as the β -phase (Al_5FeSi) and Chinese script phase π -phase ($Al_8Mg_3FeSi_6$) can also be observed. The solidification sequence is the following:

- $T = 883\text{ K } (610\text{ }^\circ\text{C})$ - Start of solidification and formation of α -Al dendrites
- $T = 841\text{ K } (568\text{ }^\circ\text{C})$ - Start of main eutectic reaction: $Liq. \rightarrow Al + Si + Al_5FeSi$
- $T = 830\text{ K } (557\text{ }^\circ\text{C})$ - Precipitation of Mg_2Si : $Liq. \rightarrow Al + Si + Mg_2Si$

- $T = 823 \text{ K}$ ($550 \text{ }^\circ\text{C}$)-Precipitation of complex eutectic: $\text{Liq.} \rightarrow \text{Al} + \text{Si} + \text{Mg}_2\text{Si} + \text{Al}_8\text{Mg}_3\text{FeSi}_6$
- $T = 816 \text{ K}$ ($543 \text{ }^\circ\text{C}$) – Solidus

According to Arnberg et al. [2], the nucleation of α -Al starts at 610°C . Equiaxed dendritic crystals begin to grow, and become coherent at 604°C . The eutectic reaction starts at 568°C , and the Al-Si eutectic phase and the first β - Al_5FeSi crystals appear. As solidification goes on, the Mg_2Si phase and the π - $\text{Al}_8\text{Mg}_3\text{FeSi}_6$ phase precipitate.

Heat treatments are applied to Al-Si alloys to increase their mechanical properties. According to Belov [3], the T6 heat treatment is one of the most used for the A356 alloy.

During the first step (solutionising: at $540 \text{ }^\circ\text{C}$ for 4 h), phases like π - $\text{Al}_8\text{Mg}_3\text{FeSi}_6$ and Mg_2Si progressively dissolve. Another important aspect is the change in shape of the eutectic Si crystals from plate-like to globular, which leads to an increase in the ductility of the alloy. The alloy is then rapidly cooled in order to obtain a highly supersaturated solid solution rich in vacancies.

The alloy is finally aged to form strengthening intermediate phases within the aluminium matrix, which hinder the movement of dislocations. Typical artificial ageing temperatures are in the range $150 \text{ }^\circ\text{C}$ to $250 \text{ }^\circ\text{C}$, and artificial ageing times can be as long as 12 h.

1.2 The influence of Ni

Nickel is added to aluminium foundry alloys to increase the mechanical properties, especially at elevated temperatures.

Granfield et al. [4] studied the addition of Ni as trace element (300 ppm) in a AA6063 and A356 alloys, but they found out that it had almost no influence on the mechanical and corrosion properties.

Zhu et al. [5] added from 80 to 500 ppm to A356 alloy and the mechanical properties and results were in good agreement with Granfield's work.

García [6] found out that 0.5 and 1 wt% Ni additions to an Al-7wt% Si alloy decrease strength, elongation and hardness because of the formation of brittle Al_3Ni particles.

Ludwig [7] added 300 and 600 ppm Ni to a commercial purity A356 alloy and observed that two principal intermetallic phase had formed: Al_3Ni was found in the immediate proximity of eutectic

Si, whereas Al_9FeNi intermetallics had a compact shape and could be observed close to the π -phase.

Casari et al. [8] reported that the addition of 600 ppm Ni addition strongly influences the tensile properties of the as-cast A356 alloy, reporting a reduction of the UTS and $R_{p0.2}$ of 87% and 37%, respectively. Ni-rich intermetallics were observed in the fracture surface and were found to fracture more easily than other secondary phases.

Ashgar et al. [9] reported significant elevated temperature strength in Al-12SiNi alloy. The addition of 1.2wt% Ni led to the formation of an interconnected hybrid reinforcement consisting of eutectic Si and Ni- and Fe-containing intermetallic phases.

Also Heusler et al. [10] presented a new alloy for engine applications based on the Al-Si-Mg-Cu-Fe-Ni system with increased fatigue properties (+20%) and tensile strength with respect to Al-Si based alloy. This increase was attributed to the presence of Ni-bearing intermetallic compounds.

2. Materials and Methods

2.1 Preparation of the alloys

A commercial purity A356 alloy was used as base material. The ingots were melted in a boron-nitride coated clay-graphite crucible at 740 °C. Ni was added to the melt according to the targeted nominal concentrations of 0.5, 1 and 2 wt% using an Al-10 wt% Ni master alloy, holding for 10 min to have complete dissolution. According to the EN AB-42100 specification for the A356 alloy, the level of Si should be in the range 6.5 - 7.5 wt%. Hence, pure Si was added to the melt aiming at an average level of 7 wt% Si. The melting furnaces used in the experimental work crucibles are shown in Figure 1.

Melts were then degassed with argon gas for 10 min just prior to casting. Permanent mould castings were obtained by pouring the molten alloy into a L-shaped preheated steel mould manufactured according to the UNI 3039 specification. The temperature of the die was kept at 573 K (300 °C) during the casting trials.



Figure 1- The melting furnaces used for the experimental work

2.1.1 Chemical analysis

Glow discharge optical emission spectroscopy (GD-OES) was employed to determine and to verify the content of the alloying elements, in particular the Ni levels.

GD-OES is a mature and versatile technique for the direct determination of trace elements in a variety of materials. The technique is an extension of the earliest forms of mass spectrometry. Processes inherent to the glow discharge optical emission spectroscopy, namely cathodic sputtering coupled with Penning ionization, yield an ion population from which semi-quantitative results can be directly obtained [5].

Sample for GD-OES analysis were ground using SiC papers from 80 up to 500 grit (Figure 2). Three different specimens for each Ni additions were examined. The measured chemical compositions of the alloys are reported in Table 2



Figure 2 - Specimens for GD-OES analysis.

Alloy		Si	Ni	Fe	Al
A356 + 0.5	wt%	6.932	0.413	0.083	82.95
	Rsd (%)	1.04	3.87	5.23	0.41
A356 + 1,0	wt%	6.721	0.889	0.078	83.92
	Rsd (%)	1.41	5.42	5.89	0.56
A356 + 2.0	wt%	6.910	1.847	0.076	81.75
	Rsd (%)	2.75	1.30	1.98	0.99

Table 2 - Chemical composition (wt%) of the Ni-containing A356 alloys as measured by GD-OES.

2.1.2 Thermal analysis

Thermal analysis was used for predicting the quality of the prepared aluminium alloys and for determining the thermal parameters associated with nucleation of α -Al dendrites and the eutectic mixture. Specimens for thermal analysis were cast for each Ni addition. The alloys were poured in a preheated graphite mould and a K-type thermocouple was lowered centrally into the liquid metal to record the temperatures during solidification. A Fiberfrax board was placed on top of the crucible and the melt was left cooling in ambient air. A sampling frequency of 50 Hz was set in the data logger. The system used for recording data is shown in Figure 3

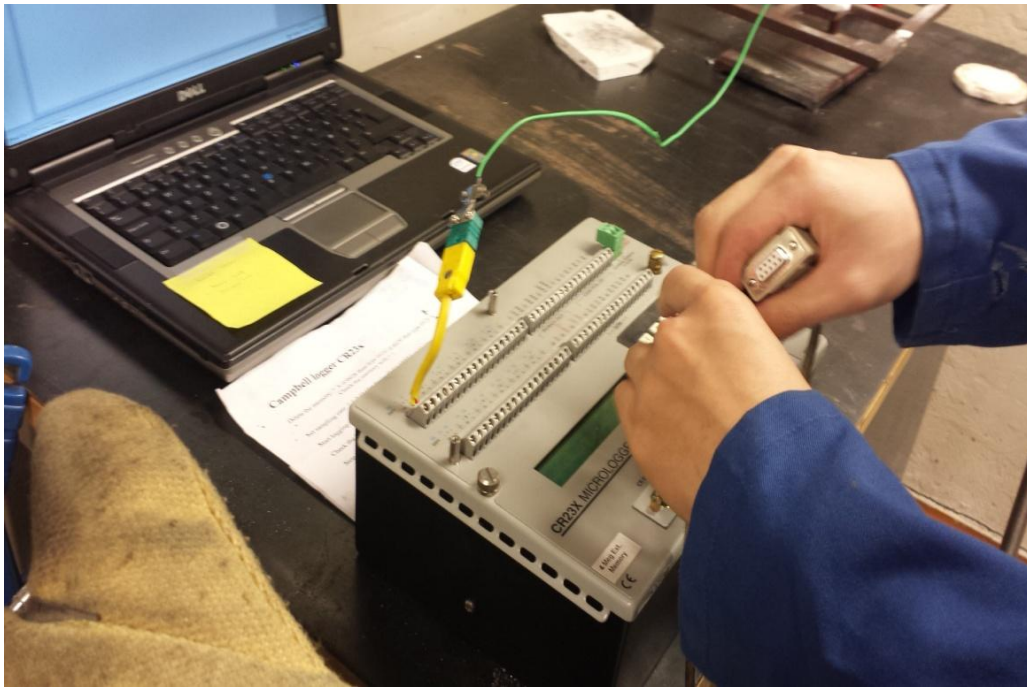


Figure 3 - The data logger used for sampling temperature-time data during solidification

Several solidification curves were obtained for each addition. All the curves were evaluated and compared by setting the x-coordinate (time) from 0 to 40 sec, the y-coordinate (temperature) from 700 °C to 500 °C. The first derivatives of the curves were also studied and their peaks were examined. To obtain the characteristic solidification parameters of the alloys, the method of Tamminen was used [1,7] (Figure 4). Several parameters were thus extracted from the cooling curves for the α -Al primary phase and the eutectic phase, such as the nucleation (T_N) and growth (T_G) temperatures, the minimum nucleation temperature (T_{min}) and the recalescence (ΔT_R). Finally, the solidus temperature (T_S) and the solidification interval (ΔT_S) were determined.

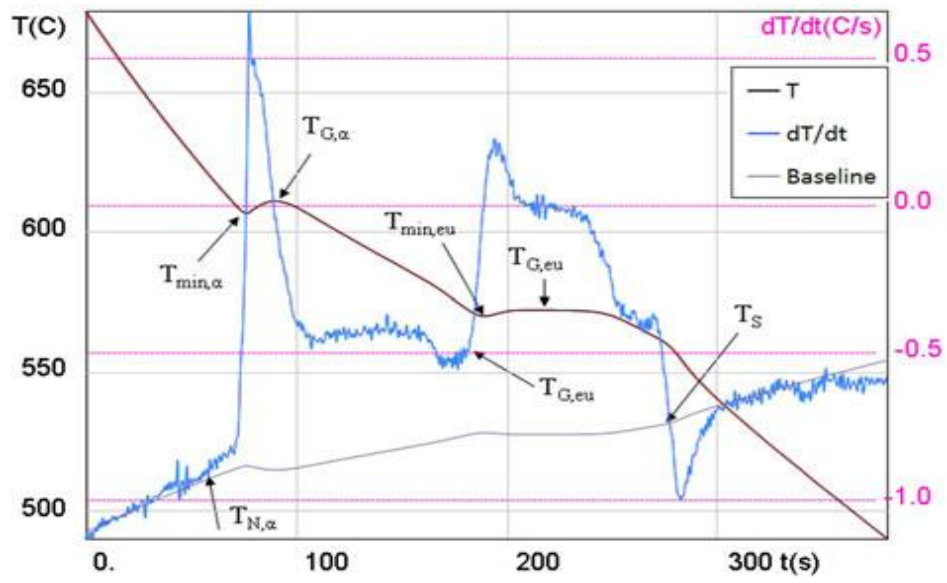


Figure 4 – Typical solidification curve, associated first derivative, and baseline of a binary Al-Si alloy. [7]

2.2 Preparations of the samples

2.2.1 Casting and T6 Heat Treatment

As mentioned previously, permanent mould castings were obtained by pouring the molten alloy into a L-shaped preheated steel mould. A number of thirty castings were obtained, ten for each Ni addition.

Half of the castings was then subjected to a T6 heat treatment consisting of three different stages:

- Two step solutionising: at 520 °C for 2 h and 540 °C for 2 h;
- Quenching in a water bath at 20 °C;
- Aging at 160 °C for 6 h.

The two steps solutionising was carried out to prevent incipient melting of the eutectic regions. In total, a number of six different experimental conditions were investigated (Table 3).



Figure 5 – Furnace used for the heat treatment.

Alloy	Condition	Alloy Code
A356 + 0.5 wt% Ni	As cast	Ni 0.5 – AC
	T6	Ni 0.5 – T6
A356 + 1 wt% Ni	As cast	Ni 1 – AC
	T6	Ni 1 – T6
A356 + 2 wt% Ni	As cast	Ni 2 – AC
	T6	Ni 2 – T6

Table 3- The casting plan

2.2.2 Machining of the tensile and Charpy impact samples

In accordance with the UNI EN ISO 6892-1 specification for the high-temperature tensile tests and with the UNI EN ISO 14556 for notched (A-type) Charpy impact test, specimens were machined as reported in Figure 6, Figure 7 and Table 4, Table 5.

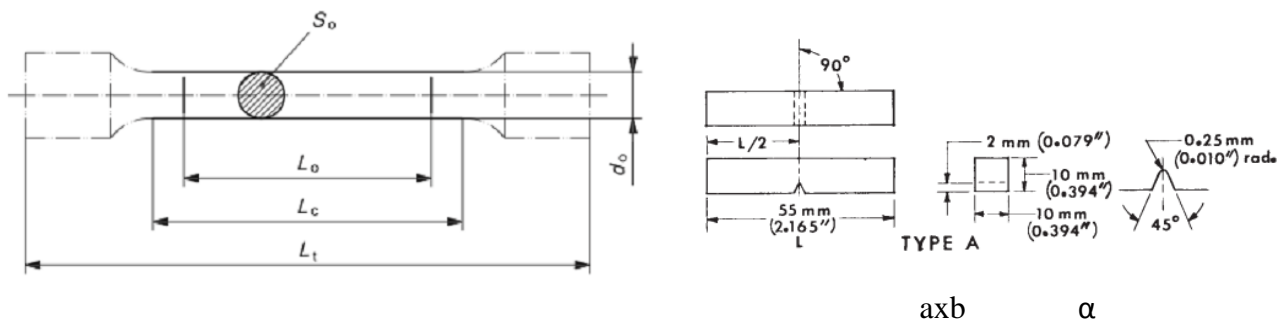


Figure 6 - Tensile and notched (A-type) Charpy impact specimens.

For the elevated temperature tensile specimens:

Diameter of the parallel length	$d_0 = 6 \text{ mm}$
Gauge length	$L_0 = 40 \text{ mm}$
Parallel length	$L_C = 70 \text{ mm}$
Diameter of grip section	$d = 10 \text{ mm}$
Total length of test piece	$L_T = 135 \text{ mm}$
Transition radius	$R = 60 \text{ mm}$

Table 4 - Machining parameters for the elevated-temperature tensile specimens

For the notched (A-type) Charpy impact specimens:

Adjacent sides shall be at:	$\beta = 90^\circ$
Transverse section	$a \times b = 10 \times 10 \text{ mm}$
Length of specimen	$L = 55 \text{ mm}$
Depth of notch	$p = 2 \text{ mm}$
Angle of notch	$\alpha = 45^\circ$
Radius of notch	$r = 0,25 \text{ mm}$
Surface finish on the notched surface and the opposite one	$R_{a,1} = 2 \text{ } \mu\text{m}$
Surface finish on the other 4 facets	$R_{a,2} = 4 \text{ } \mu\text{m}$

Table 5 - Machining parameters for the notched (A-type) Charpy impact specimens.

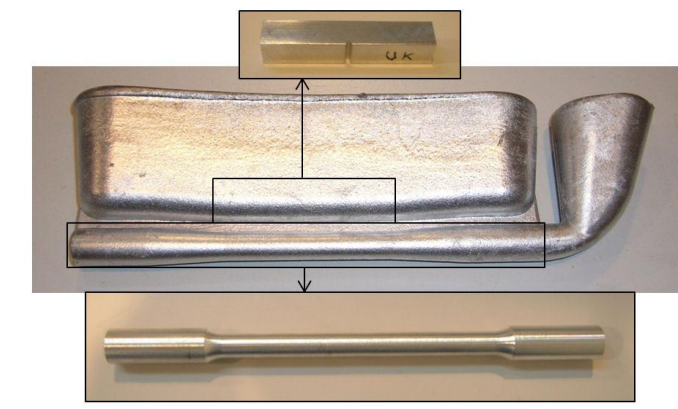


Figure 7 – Regions from which the tensile and the notched (A-type) Charpy impact specimens were obtained.

2.3 High-temperature tensile tests

Tensile specimens were tested in accordance with the ISO 6892-2 specification using an MTS 880 universal testing machine (10 tons) equipped with a furnace chamber and a MTS Teststar control unit (Figure 8 and 9). Temperature in the furnace chamber was set at 508 ± 5 K (235 ± 5 °C). All the as-cast and T6 heat-treated samples were kept at the pre-set temperature for 15 min before testing to ensure a homogeneous temperature. Tensile tests were carried out at a crosshead speed of 1 mm/min and with the applied load restricted to 40 kN. A specifically designed clip-on stainless steel axial extensometer connected to an optical position measuring system was used to collect stress-strain data. At least five samples were tested for all the six experimental conditions.

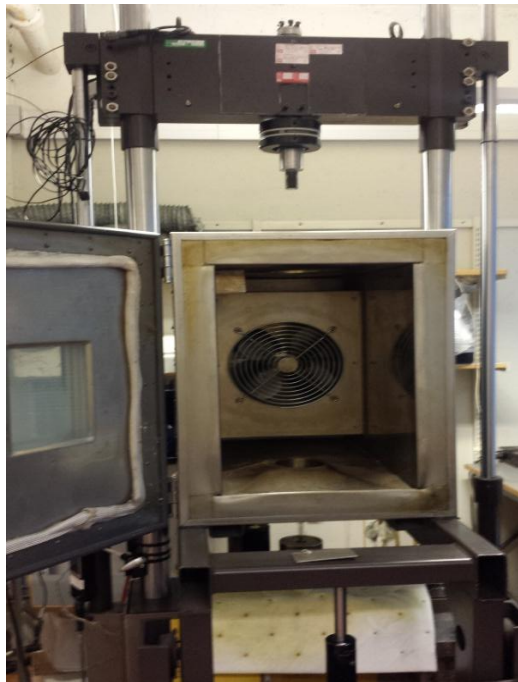


Figure 8 – The high-temperature tensile testing machine.

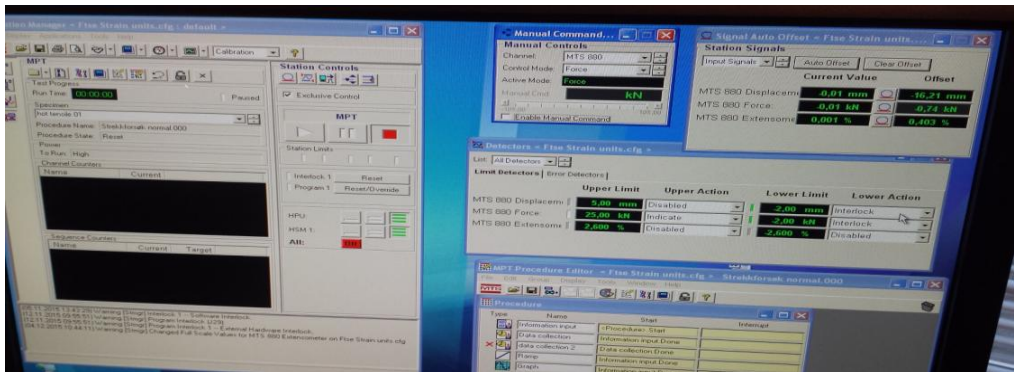


Figure 9 - The software utilised to obtain the stress-strain curves.

2.4 Charpy Impact tests

In accordance with the ASTM E-23 specification, a Charpy pendulum was utilised for impact tests. Similarly to tensile tests, five samples were tested for each experimental condition. The data was acquired by a DAS 64000 analyser, which allowed to record the load-deflection curve. The total absorbed energy (W_t) was then calculated as the integral of the load-displacement curve. Other parameters such as crack initiation (W_m) and crack propagation energies (W_p) as well as the maximum load required to break the specimens (F_{max}) were calculated

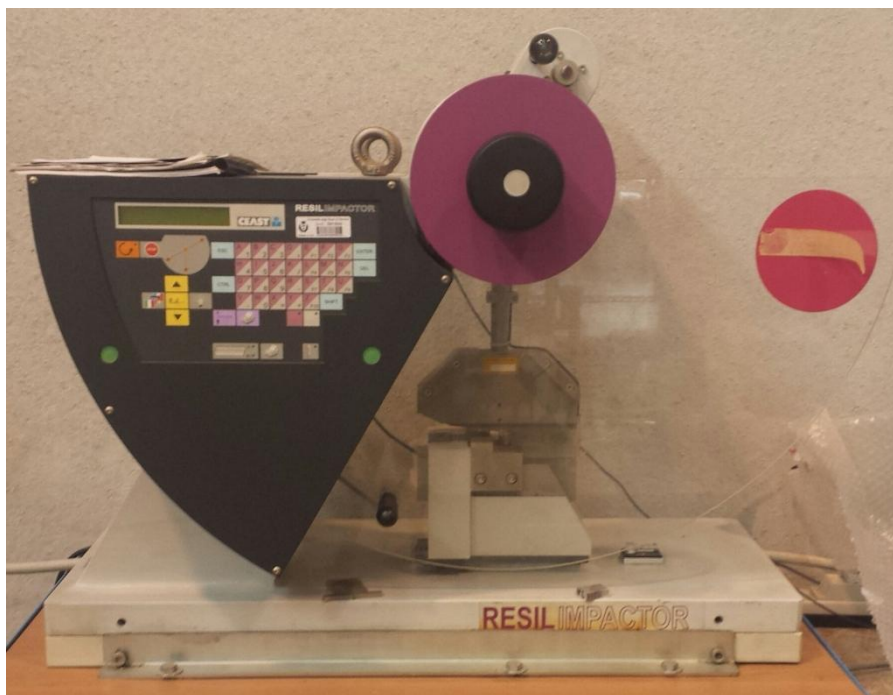


Figure . Charpy pendulum

2.5 Microstructural analysis

Samples for microstructural investigations were cut from the tensile specimens, embedded in phenolic resin and prepared using standard grinding (SiC papers up to 1200 grit) and polishing (alumina suspensions) procedures. Microstructural analysis was performed using a LEICA MEF4M optical microscope (OM). Also SEM analysis was performed. No etchants were employed.



Figure 10 – Samples for microstructural analysis showing the fracture profiles of the tensile specimens.

3. Results

3.1 Characteristic temperatures

The average values of the characteristic solidification parameters for each Ni addition are reported in Table 6. It was observed that the nucleation temperature for the α -Al phase in Ni 0.5 is 616.1 °C, for Ni 1 is 616.4 °C and for Ni 2 is 616.3 °C.

As for the eutectic Al-Si phase, the nucleation temperature is 566.9 °C for the Ni 0.5 alloy, 564.9 °C for Ni 1 and 562.6 °C for Ni 2. Thus, it is observed that the addition of Nickel decreases the nucleation and growth temperature of the eutectic Al-Si phase.

Contrarily to that, the temperature for nucleation and growth of the α -Al phase remains unchanged.

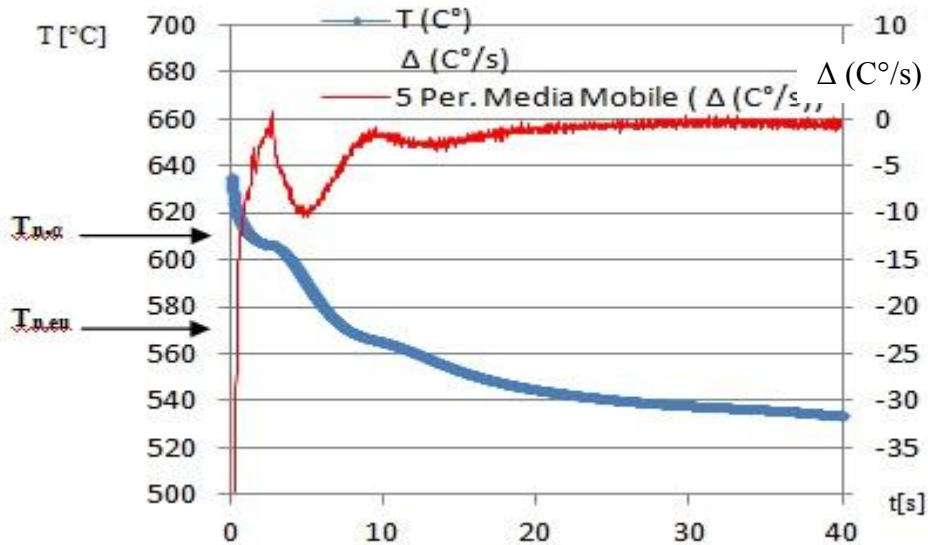


Figure 11 – Representative solidification curve for an A356 alloy added with 0.5 wt% Ni.

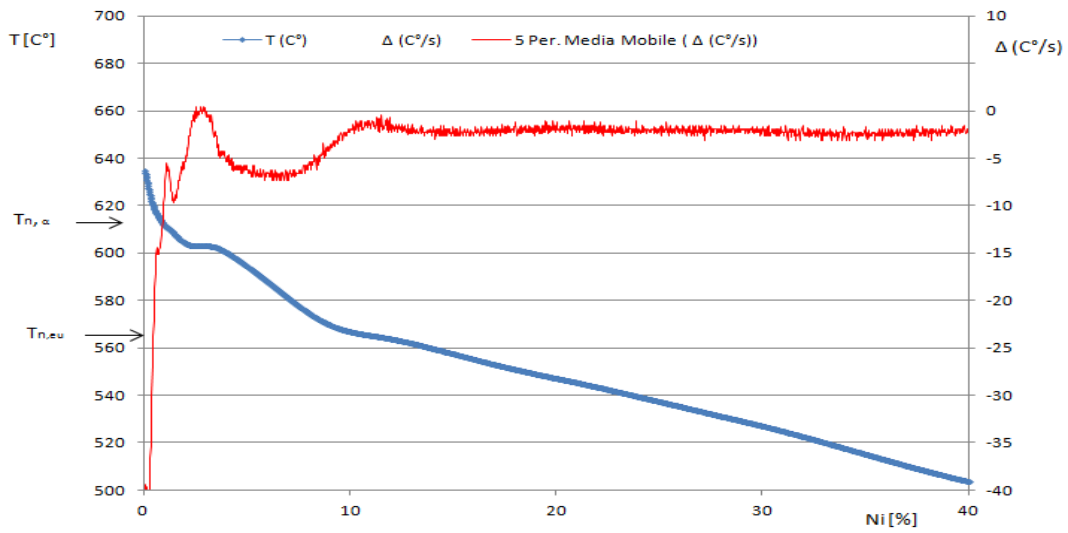


Figure 12 - Representative solidification curve for an A356 alloy added with 1 wt% Ni.

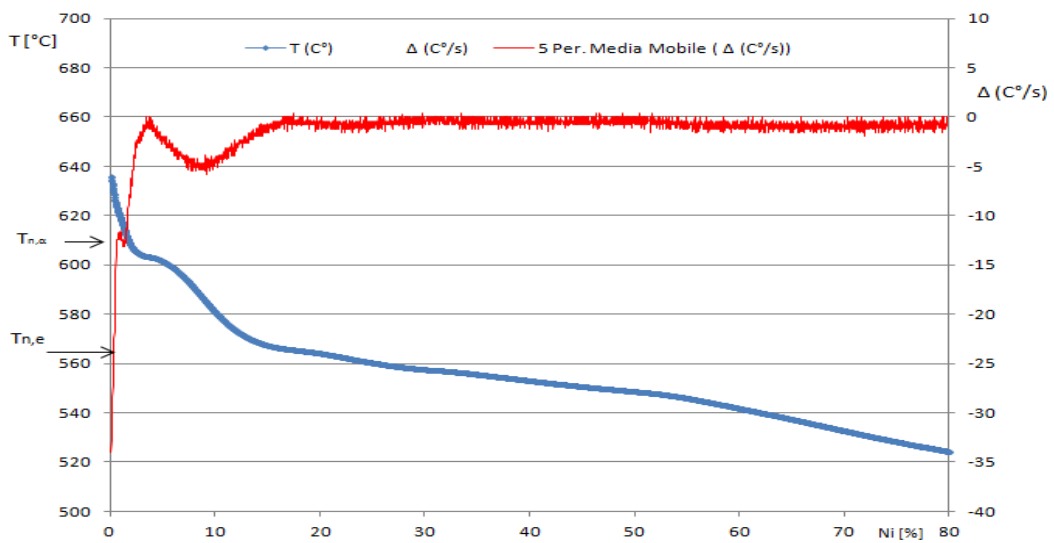


Figure 13- Representative solidification curve for an A356 alloy added with 2 wt% Ni.

Alloy	T_{n,a} [°C]	T_{min,a} [°C]	ΔT_{Ra}	T_{G,a} [°C]	T_{n,eu} [°C]	T_{min,eu} [°C]	ΔT_{Reu}	T_{G,ε} [°C]	T_s [°C]	ΔTs
Ni 0.5	616.1	607.2	1.3	608.6	567.0	568.2	1.0	569.2	548. 1	68.0
Ni 1	616.4	608.2	1.0	609.3	565.0	563.8	0.9	564.8	546. 5	70.0
Ni 2	616.3	612.0	1.1	613.0	562.6	561.3	1.4	562.8	549. 6	66.7

Table 6 - Characteristic temperatures of the Ni-containing A356 alloys

3.2 High-temperature mechanical properties

The average values of the tensile properties of the different Ni-containing alloys are summarised in Table 7.

Alloy	R_{p0.2} [MPA]	UTS [MPA]	A [%]
A356 – AC	109.6 ± 3.3	133.2 ± 4.8	3.9 ± 1.0
A356 – T6	185.7 ± 4.0	195.0 ± 3.5	3.9 ± 1.8
Ni – AC	117.2 ± 7.2	135.8 ± 6.5	2.7 ± 0.8
Ni – T6	186.0 ± 2.5	196.8 ± 2.5	4.1 ± 2.0
Ni 0.5 – AC	105.5 ± 4.0	129.4 ± 5.0	4,3 ± 1.6
Ni 0.5 – T6	180.3 ± 7.0	186.5 ± 4.0	3.2 ± 1.9
Ni 1 – AC	111.7 ± 11.0	138.4 ± 6.0	3.7 ± 0.1
Ni 1 – T6	120.8 ± 5.0	135.2 ± 4.0	3.7 ± 1.1
Ni 2 – AC	109.2 ± 5.0	134.2 ± 7.0	2.4 ± 0.4
Ni 2 – T6	114.6 ± 3.0	128.2 ± 3.0	5.3 ± 1.7

Table 7 – High-temperature mechanical properties of the Ni-containing alloys in as cast and T6 heat treated conditions. Tensile data for the A356 base alloy (A356 – AC/T6) and the 600 ppm Ni-containing alloy (Ni – AC/T6) are also reported [8].

As compared with the base alloy (A356 – AC/T6) and, to some extent, to the alloy containing Ni as trace element (Ni – AC/T6), the addition of 0.5 wt% Ni increases the A by 10% in as-cast and decreases by 22% in T6 conditions, respectively, whereas no noticeable changes in R_{p0.2} and UTS are observed.

The addition of 1 wt% Ni reduces A by 5% in both of the conditions. The Ni 1 – AC alloy shows slightly higher R_{p0.2} and UTS values than the corresponding base alloy. Conversely, a significant drop in such tensile properties is observed for the Ni 1 – T6 alloy (54% and 44%, respectively). The same trend can be observed for the as cast and T6 alloys having a 2 wt% Ni content. The addition of 2 wt% Ni reduces A by 26% in the as-cast condition and increases it by 36% in the T6 condition. These results are summarised in Figure 14 and Figure 15.

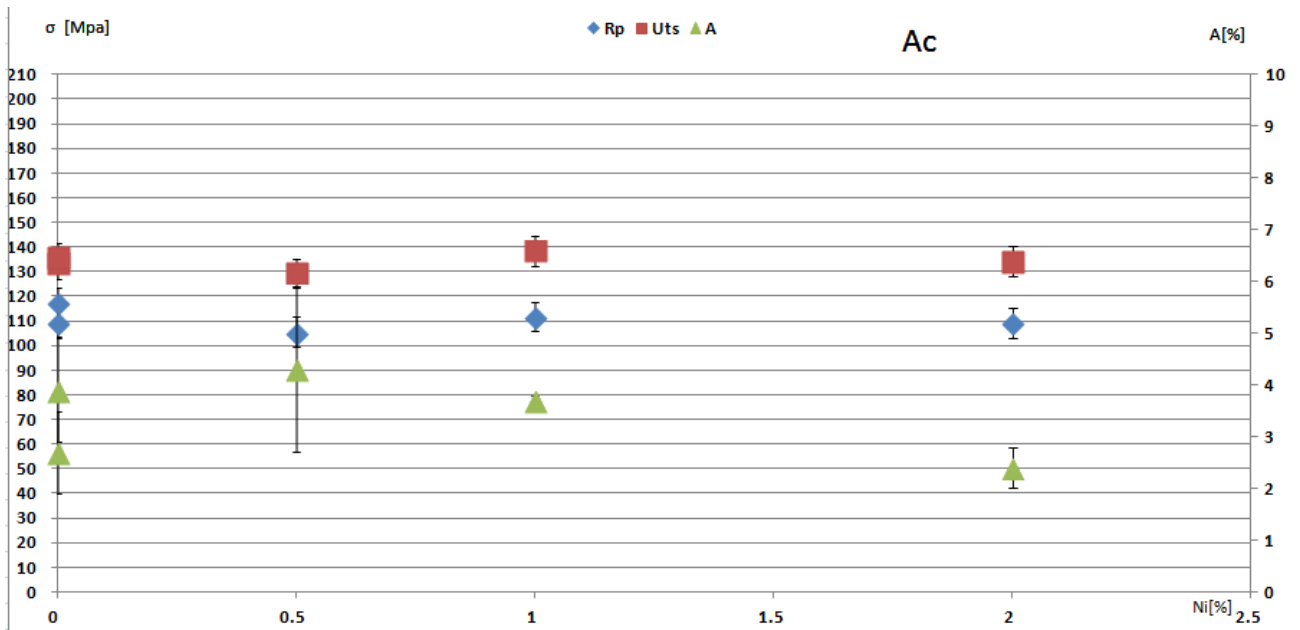


Figure 14– Effect of Ni content on the high-temperature mechanical properties of the A356 alloy in the as cast condition.

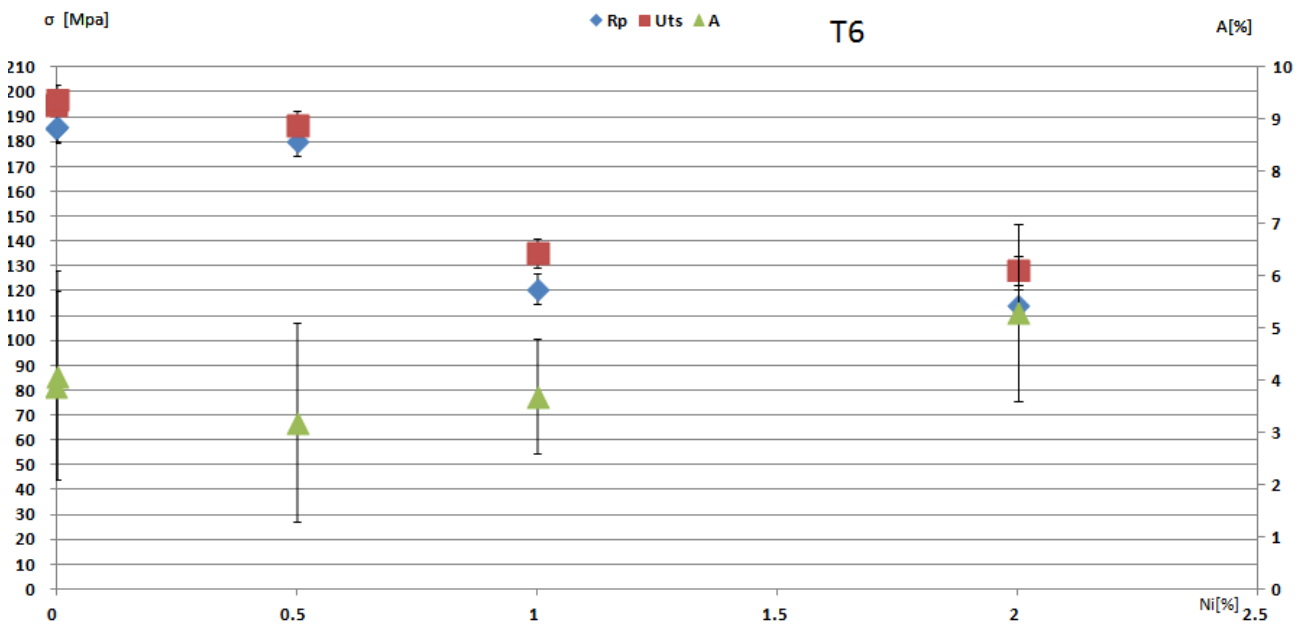


Figure 15– Effect of Ni content on the high-temperature mechanical properties of the A356 alloy in the T6 condition.

3.3 Impact properties

The average values of the impact properties of the different Ni-containing alloys are summarised in Table 8.

Alloy	Fmax [N]	Wt [J]	Wm[J]	Wp[J]
A356 – AC	3122 ± 132	1.84 ± 0.20	0.79 ± 0.07	1.05 ± 0.13
A356 – T6	4362 ± 184	1.52 ± 0.13	0.81 ± 0.09	0.71 ± 0.06
Ni – AC	2971 ± 63	1.68 ± 0.17	0.78 ± 0.02	0.91 ± 0.16
Ni – T6	4401 ± 318	1.51 ± 0.22	0.78 ± 0.10	0.73 ± 0.14
Ni 0.5 – AC	2588 ± 139	1.52 ± 0.16	0.61 ± 0.04	0.91 ± 0.15
Ni 0.5 – T6	3939 ± 106	1.29 ± 0.16	0.66 ± 0.14	0.63 ± 0.02
Ni 1 – AC	2429 ± 90	1.37 ± 0.14	0.62 ± 0.07	0.75 ± 0.07
Ni 1 – T6	3003 ± 201	1.61 ± 0.33	0.74 ± 0.19	0.87 ± 0.14
Ni 2 – AC	2448 ± 265	1.13 ± 0.14	0.51 ± 0.13	0.62 ± 0.10
Ni 2 – T6	2956 ± 239	1.25 ± 0.30	0.58 ± 0.18	0.67 ± 0.14

Table 8 - Impact properties of the Ni-containing alloys in as cast and T6 heat treated conditions. Data for the A356 base alloy (A356 – AC/T6) and the 600 ppm Ni-containing alloy (Ni – AC/T6) are also reported [11].

As compared with the base alloy (A356 – AC/T6) and, to some extent, to the alloy containing Ni as trace element (Ni – AC/T6), the addition of 0.5 wt% Ni decreases Wp by 15% and 13% in the as-cast and T6 conditions, respectively, and Wt by 22% and 18% in as-cast and T6 conditions, respectively. The addition of 0.5 wt% also decreases Fmax by 21% in the as-cast condition and increases it by 11% in the T6 condition.

The addition of 1 wt% Ni reduces Wp by 40% in the as-cast condition and increases it by 22% in the T6 condition. The Ni 1 – AC alloy shows a significantly lower Wt value than the corresponding base alloy (- 34%). A significant drop in Fmax is observed for the Ni 1 – T6 alloy (29%). The same trend can be observed for the as-cast and T6 alloys having a 2 wt% Ni content. These results are summarised in Figure 16 and Figure 17.

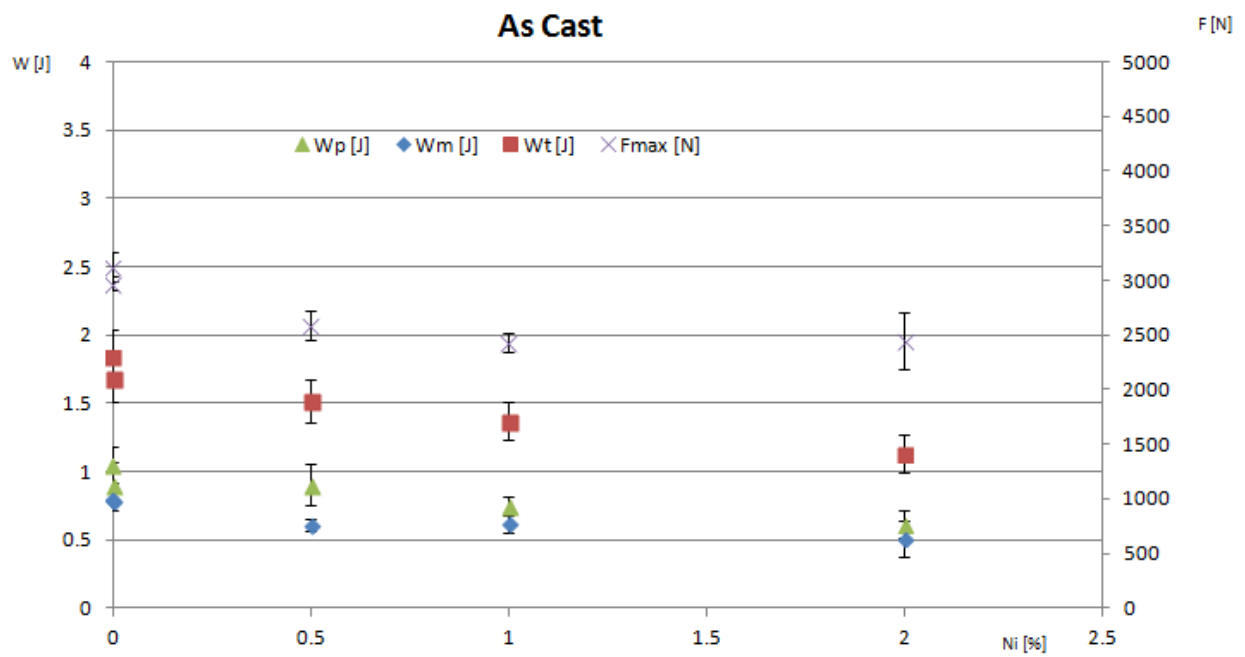


Figure 16 - Effect of Ni content on the impact properties of the A356 alloy in the as-cast condition.

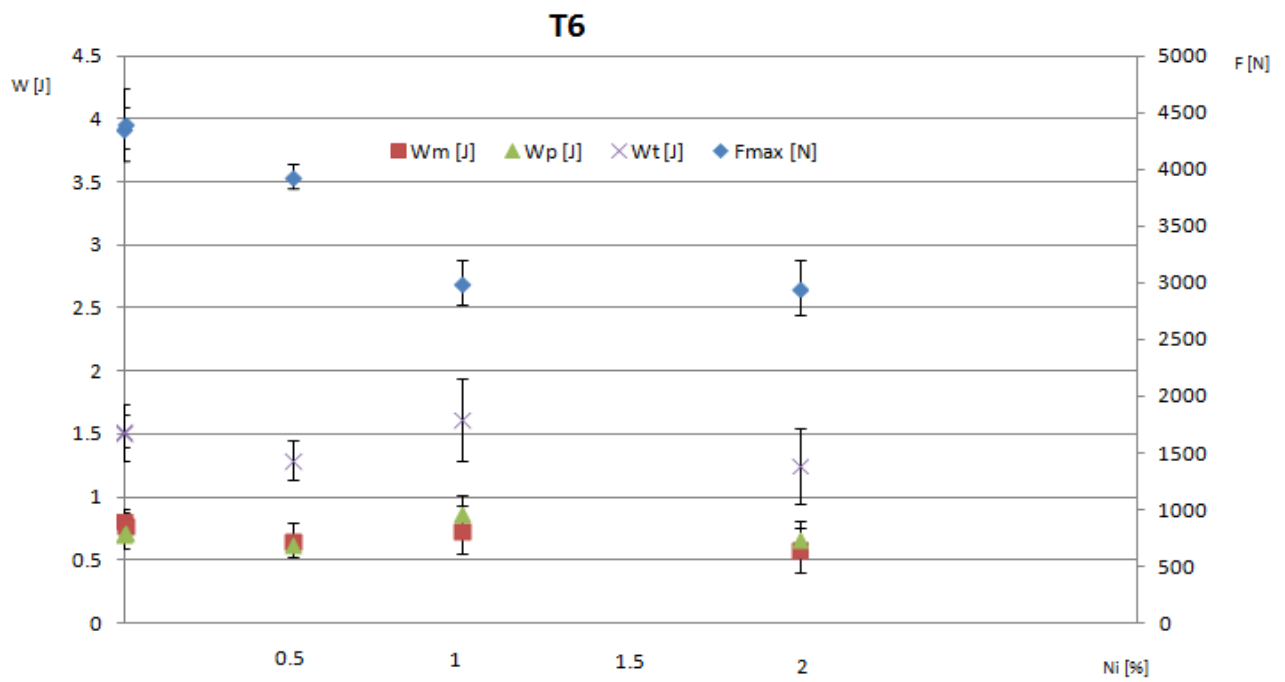
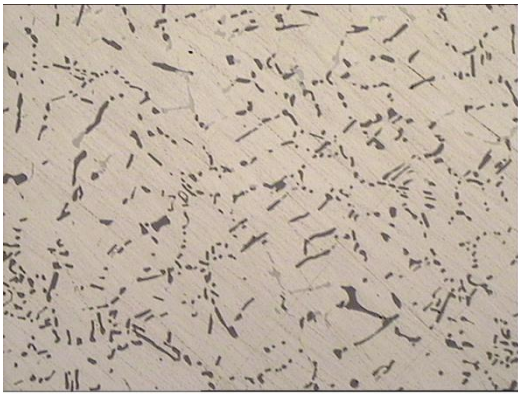


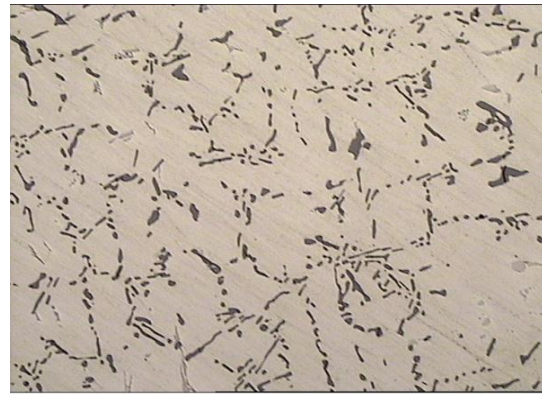
Figure 17 - Effect of Ni content on the impact properties of the A356 alloy in the T6 condition.

3.4 Microstructural investigation

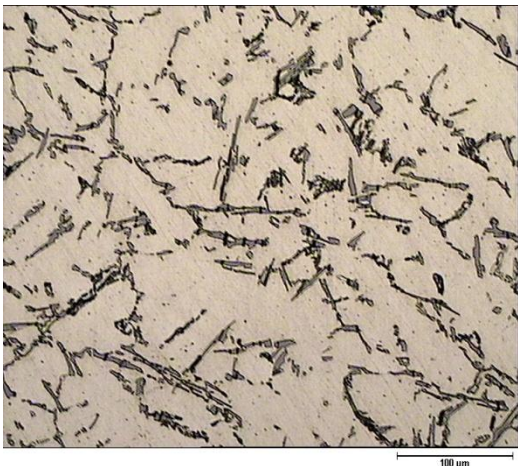
The microstructure in the as-cast condition showed α -Al dendrites and a dispersion of eutectic Si particles. After heat treatment the particles of Si separate into fragments and then spheroidise. [3] The main intermetallic phases that could be observed in the interdendritic regions were the Ni-bearing compounds (most likely the Al_3Ni phase) the Mg_2Si phase and the Chinese script π - $\text{Al}_8\text{Mg}_3\text{FeSi}_6$ phase.



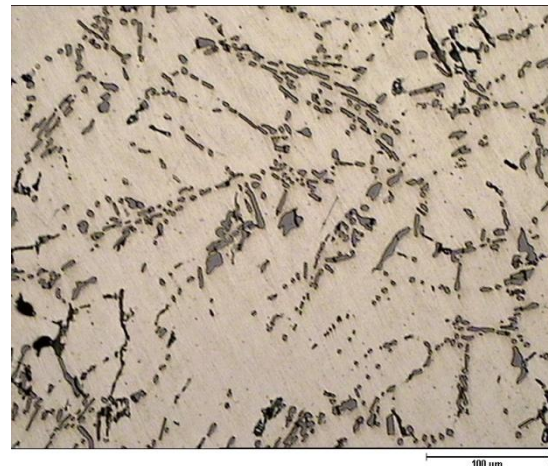
a)



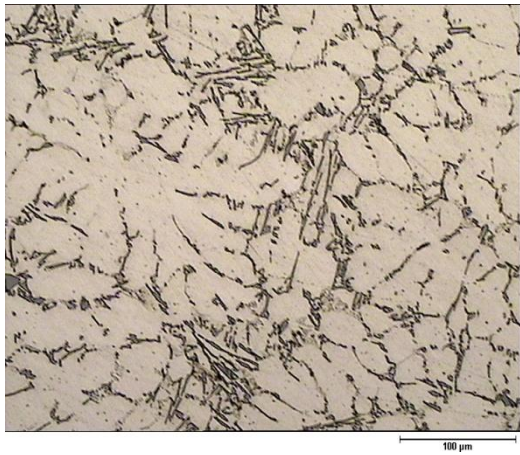
b)



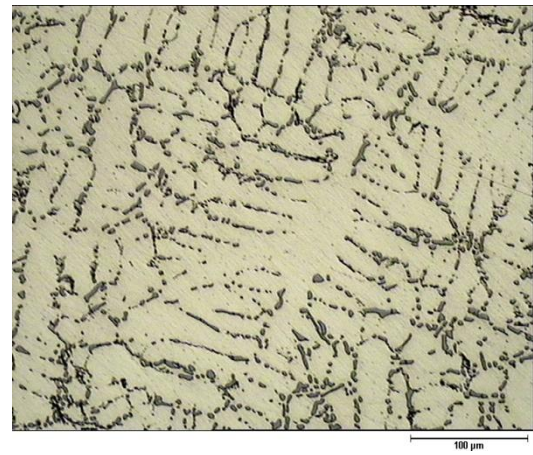
c)



d)

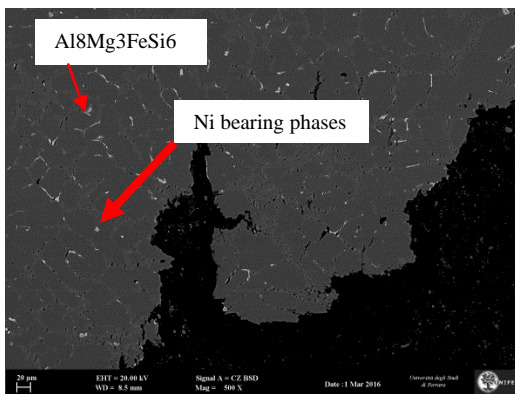


e)

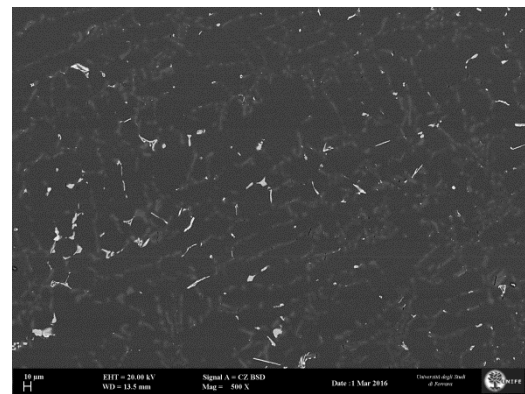


f)

Figure 18 - Microstructures of the Ni-containing alloys in the as-cast and T6 conditions. a) Ni 0.5 – AC, b) Ni 0.5 – T6, c) Ni 1 – AC, d) Ni 1 – T6, e) Ni 2 – AC, f) Ni 2 – T6.



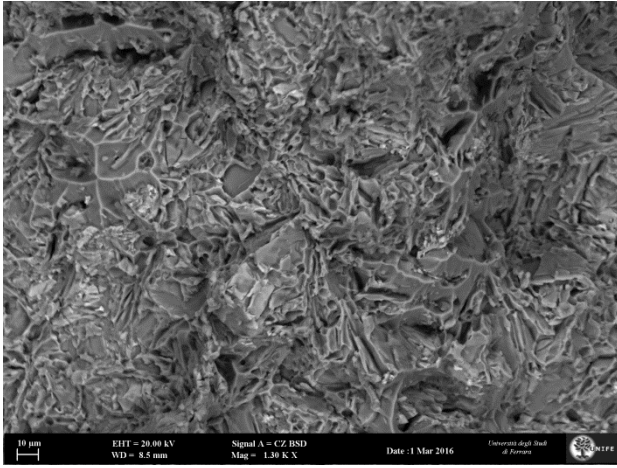
a)



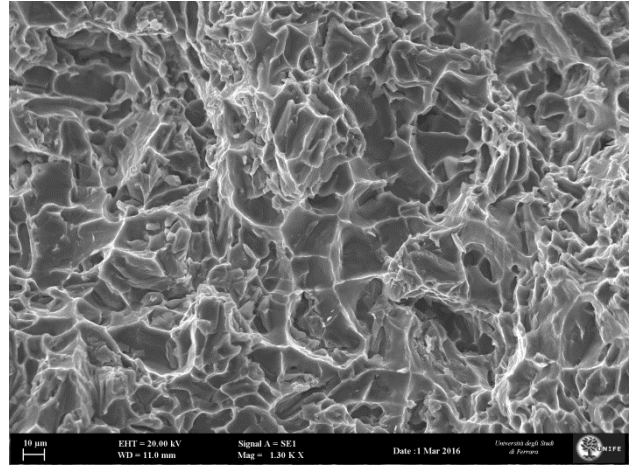
b)

Figure 19 - BSE images showing intermetallic phases in the Ni 0.5 in the a) as cast condition and b) T6 conditions

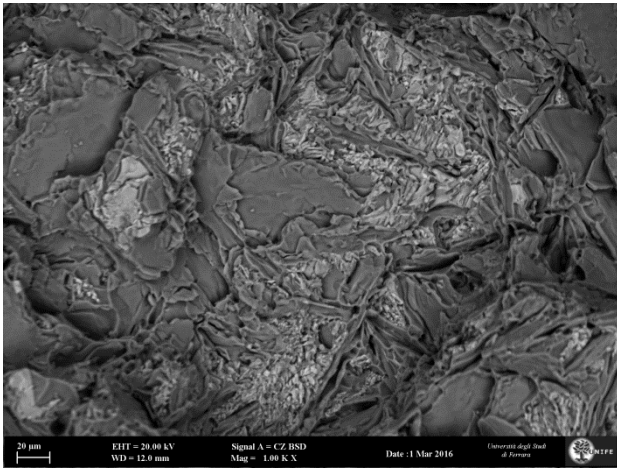
While the π - $\text{Al}_8\text{Mg}_3\text{FeSi}_6$ phase dissolved during the T6 heat treatment, the thermodynamically stable Al_9FeNi phase formed. Similarly to the eutectic Si particles, the Al_3Ni phase fragmented and spheroidised during solutionising. Intermetallic compounds are clearly distinguishable on the fracture surfaces. (Figure 20)



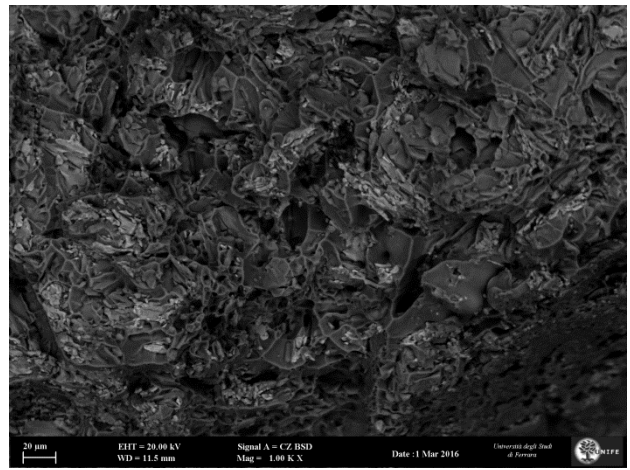
a)



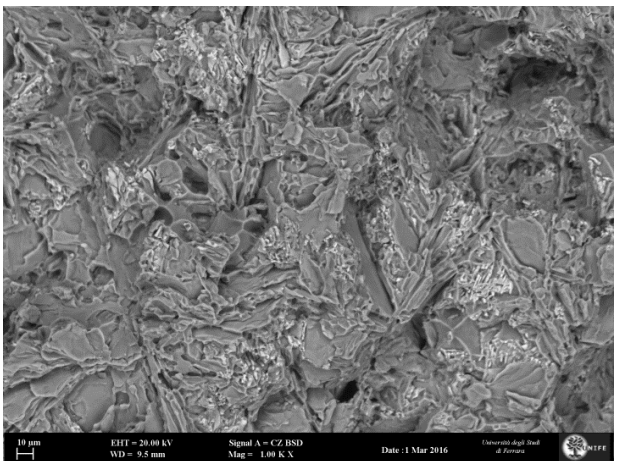
b)



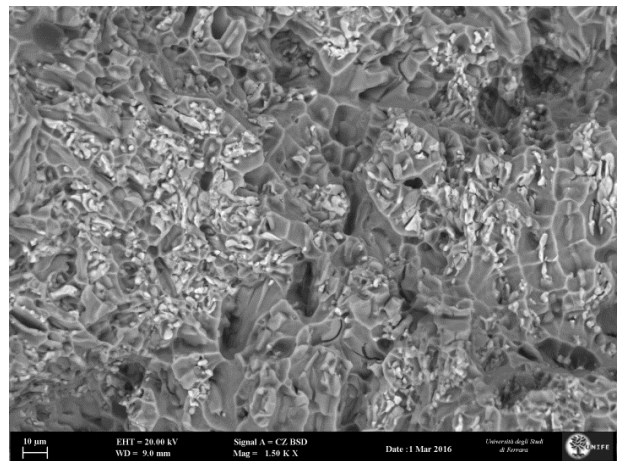
c)



d)



e)



f)

Figure 20 - SEM-BSE images of the fracture surfaces of the Ni-containing alloys. a) Ni 0.5 - AC, b) Ni 0.5 - T6, c) Ni 1 - AC, d) Ni 1 - T6, e) Ni 2 - AC, f) Ni 2 - T6.

$\pi\text{Al}_8\text{Mg}_3\text{FeSi}_6$
and Al_3Ni
phases

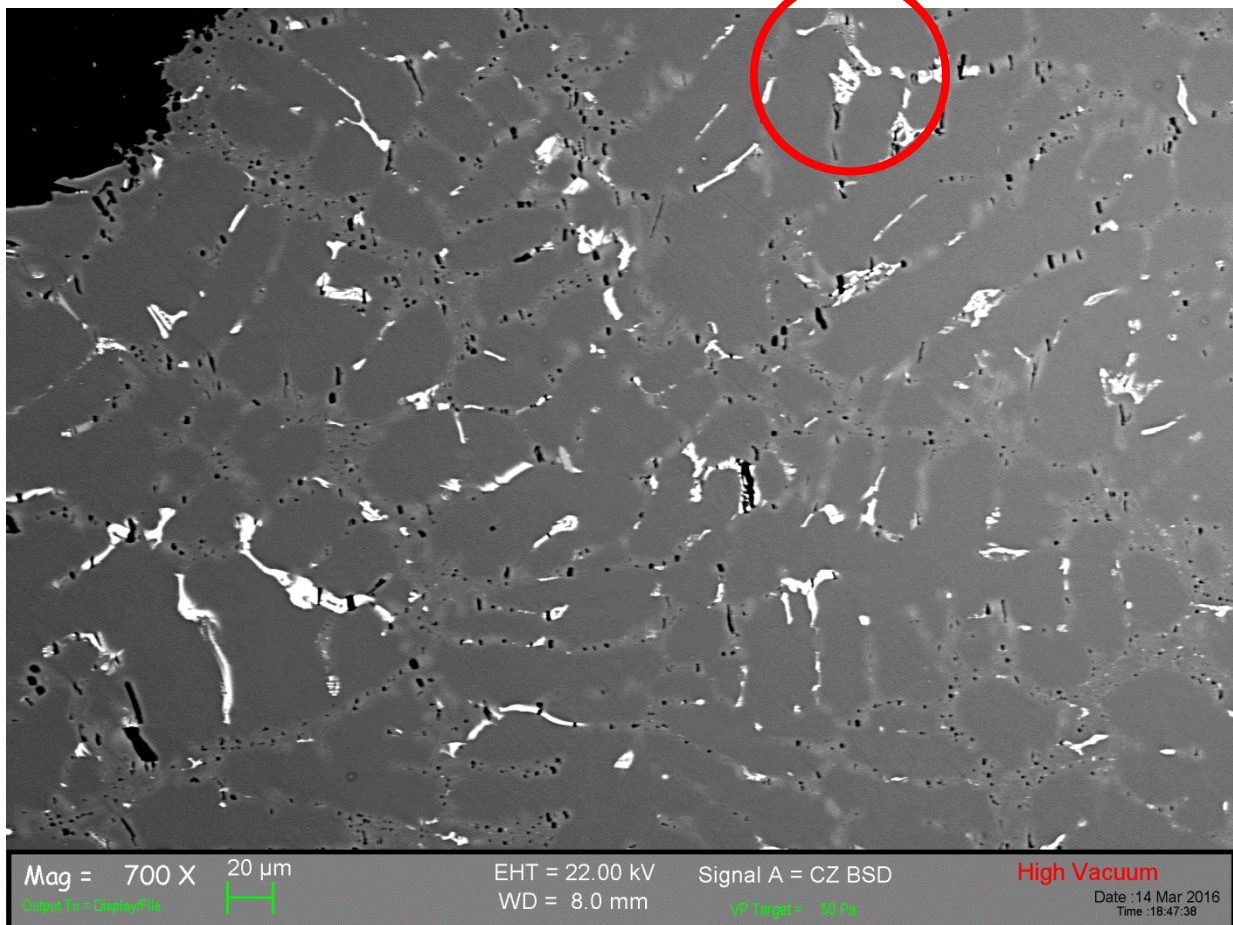


Figure 21 – $\pi\text{-Al}_8\text{Mg}_3\text{FeSi}_6$ and Al_3Ni intermetallic phases in the Ni 0.5 – AC alloy-

The resulting significant particle cracking and local linkage of microcracks along the interdendritic region seems to shape to a preferential path for transgranular crack propagation.

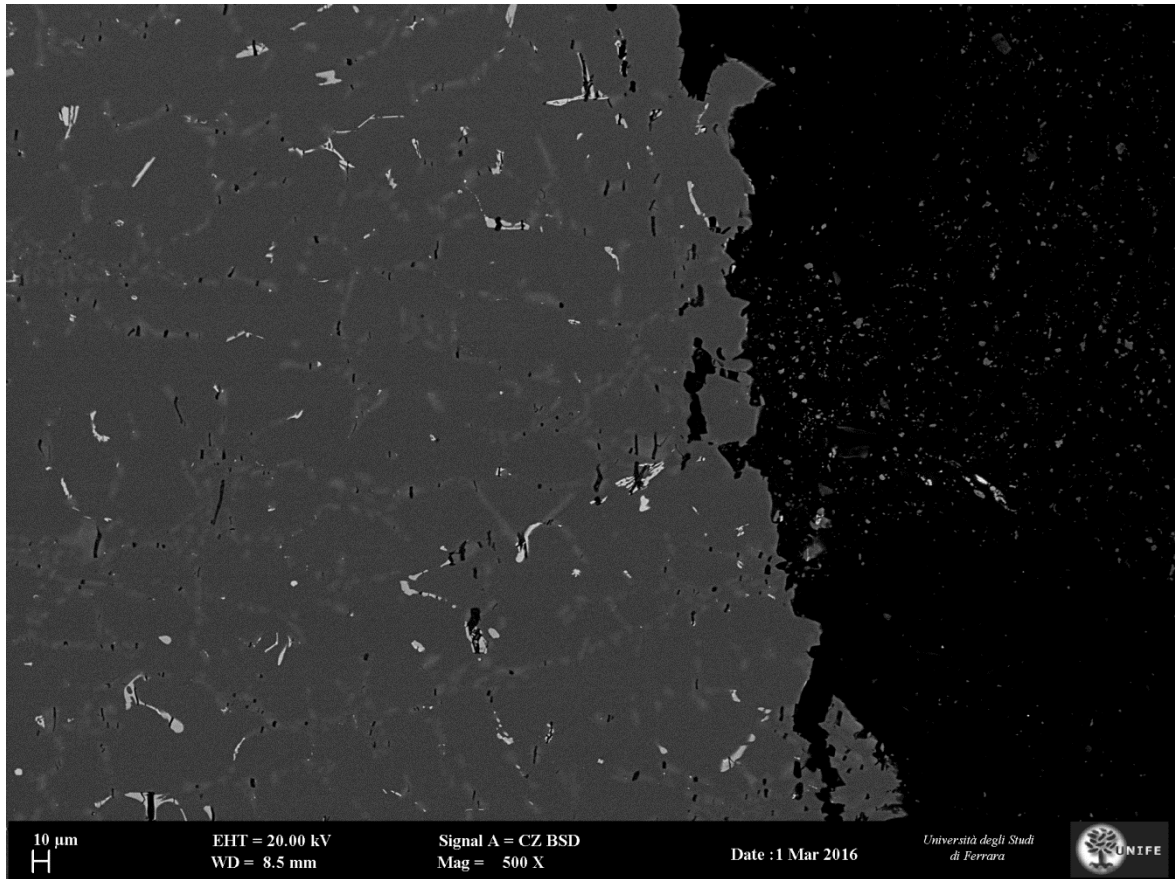


Figure 22 - BSE image of the fracture profile of the Ni 0.5 – T6 alloy.

The secondary dendrite arm spacing (SDAS) was calculated for each experimental condition. Results are collected in Table 9.

Alloy	SDAS[μm]
Ni 0.5 - AC	25.2 ± 4.2
Ni 0.5 - T6	25.8 ± 4.8
Ni 1 - AC	24.1 ± 5.7
Ni 1 - T6	24.9 ± 2.1
Ni 2 - AC	20.3 ± 12.0
Ni 2 - T6	21.3 ± 7.3

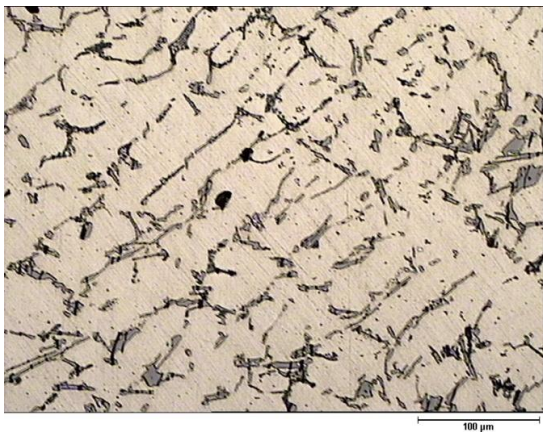
Table 9 - Average values of SDAS for each experimental condition.



a)



b)



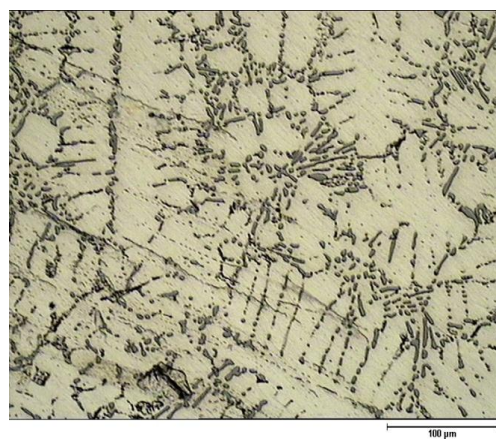
c)



d)



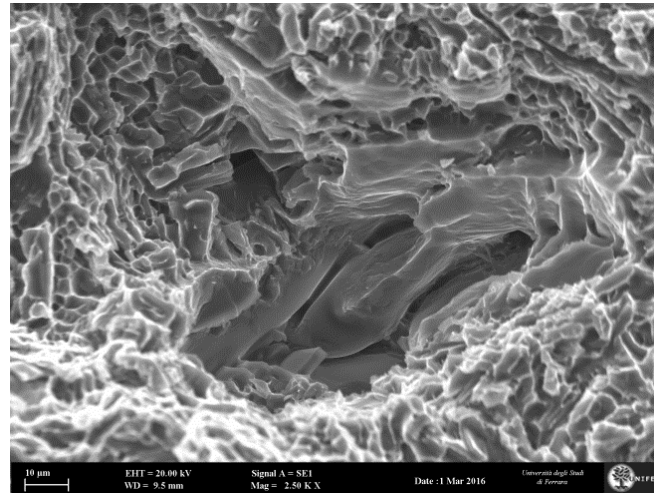
e)



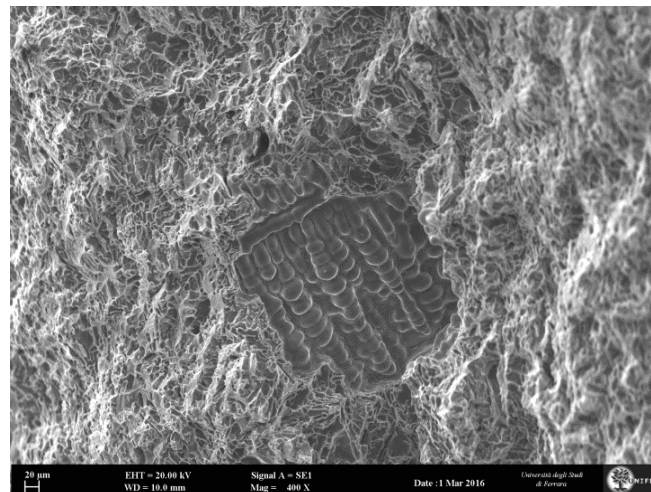
f)

Figure 23 – Representative microstructures showing the SDAS for each experimental condition: a) Ni 0.5 – AC, b) Ni 0.5 – T6, c) Ni 1 – AC, d) Ni 1 – T6, e) Ni 2 – AC, f) Ni 2 – T6.

Shrinkage defects were also detected. These defects can occur when standard feeding metal is not available to compensate for shrinkages as the thick metal solidifies (Figure 24 and Figure 25).

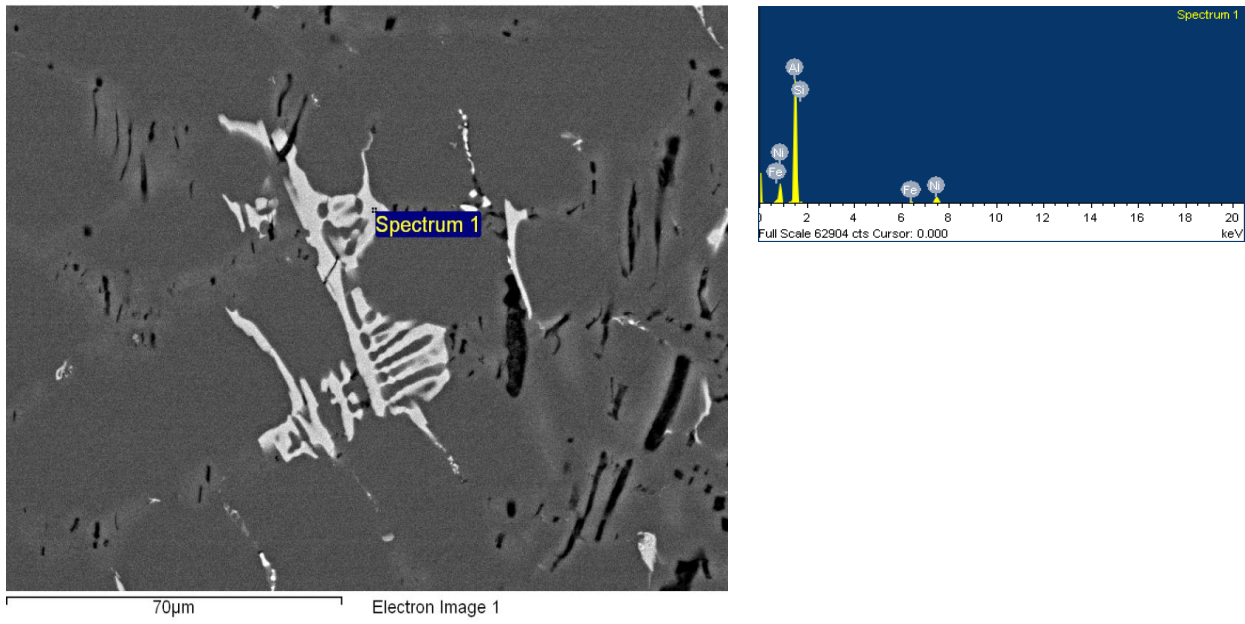


**Figure 24 – Shrinkage porosity
in Ni 0.5 As cast condition**



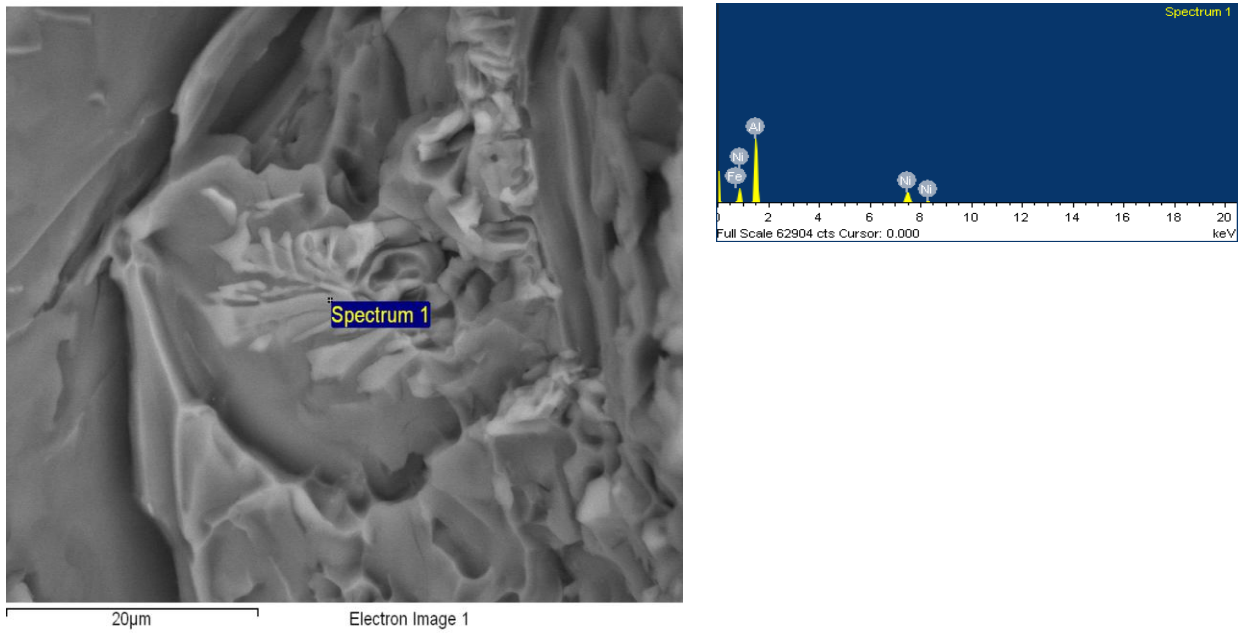
**Figure 25 - Shrinkage porosity
in Ni 0.5 - AC alloy.**

The representative chemical compositions of some of the investigated phases detected by EDS are given in Figure 26-30. The chemical compositions of the detected intermetallic phases were found to be in good agreement with the findings of previous works [3,7].



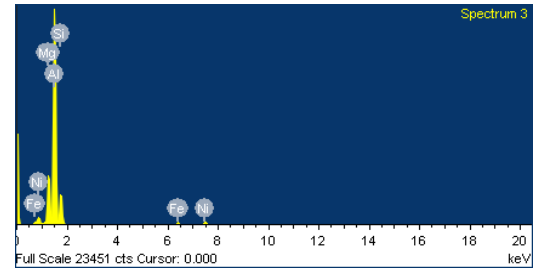
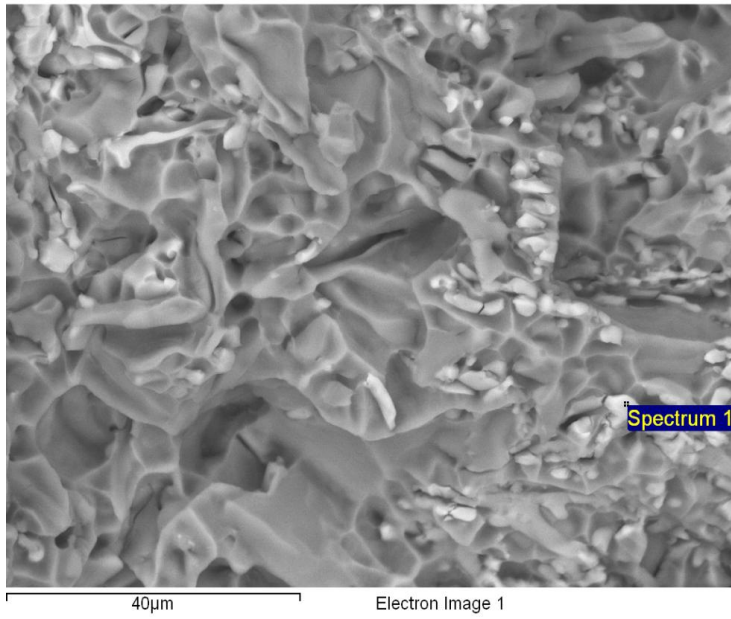
Element	Atomic [%]	Weight [%]
Al	79.33	69.76
Si	1.00	0.92
Fe	1.95	3.54
Ni	12.38	23.69

Figure 26 –BSE image of an intermetallic phase detected in the interdendritic regions of the Ni 0.5 – AC alloy. EDS measurements indicate the nature of the intermetallic compound as Al_3Ni .



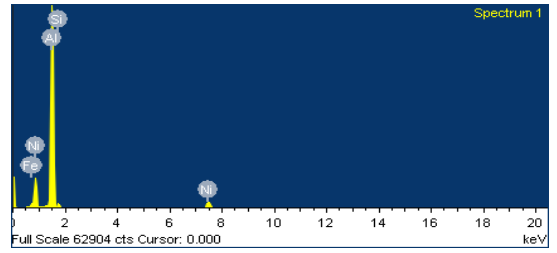
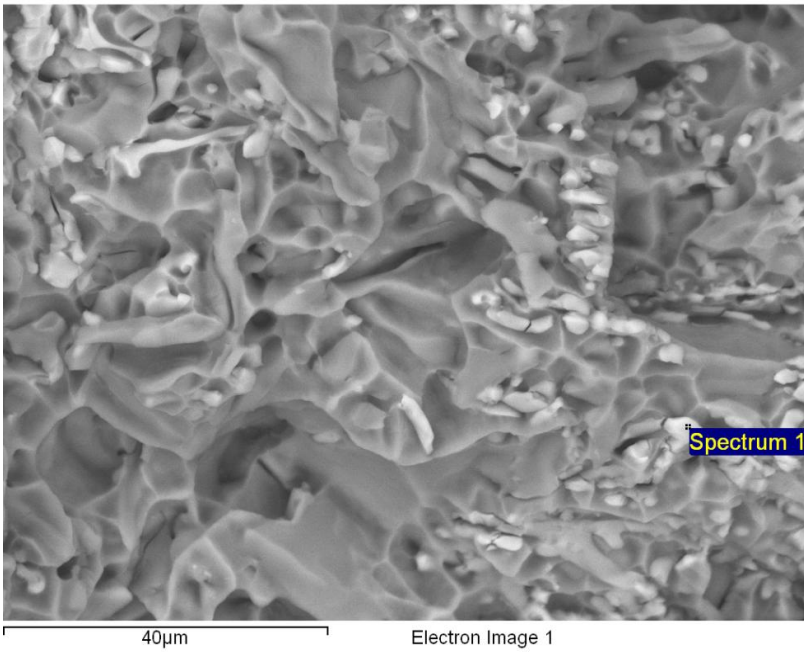
Element	Atomic [%]	Weight [%]
Al	66.93	53.26
Si	0.80	0.67
Fe	0.26	0.44
Ni	24.91	43.12

Figure 27 – BSE image of an intermetallic phase detected on the fracture surface of the Ni 0.5 - T6 alloy. EDS measurements indicate the nature of the intermetallic compound as Al_3Ni .



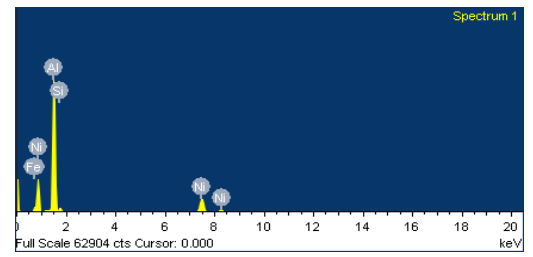
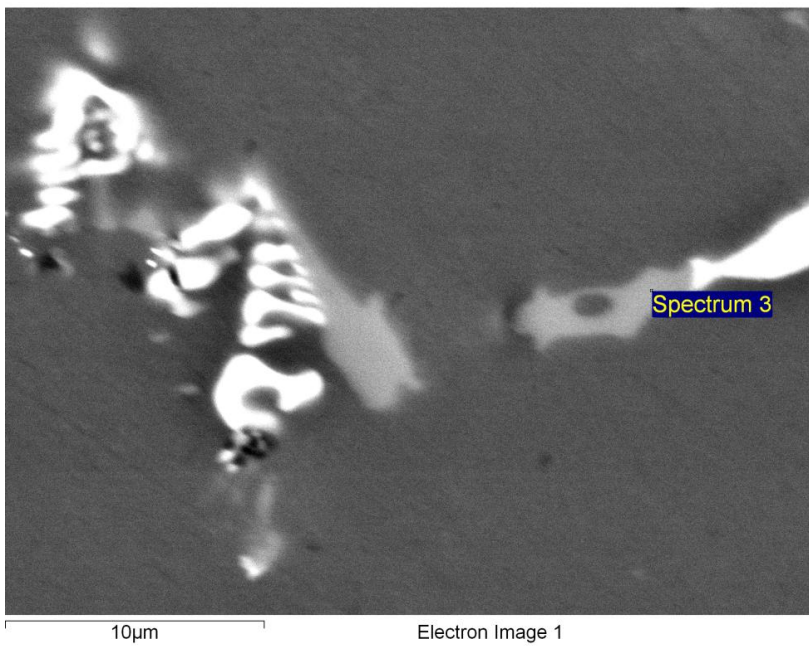
Element	Atomic [%]	Weight [%]
Al	80.97	76.13
Si	3.23	3.16
Fe	0.21	0.41
Ni	8.47	17.33

Figure 28 – BSE image of an intermetallic phase detected on the fracture surface of the Ni 2 – AC alloy. EDS measurements indicate the nature of the intermetallic compound as Al₆Ni.



Element	Atomic [%]	Weight [%]
Al	73.85	61.19
Si	2.83	2.44
Fe	0.32	0.54
Ni	19.06	34.37

Figure 29 – BSE image of an intermetallic phase detected on the fracture surface of a Ni 2 – T6 alloy. EDS measurements indicate the nature of the intermetallic compound as Al_3Ni .



Element	Atomic%	Weight%
Mg	11.85	13.59
Al	62.24	64.34
Si	18.70	18.57
Fe	2.60	1.30

Figure 30 – BSE image of an intermetallic phase detected in the interdendritic regions of the Ni 0.5 – AC alloy. EDS measurements indicate the nature of the phase as π -Al₈Mg₃FeSi₆.

4. Discussion

The results of the present work can be compared to Stadler's investigation [12], where AlSi7 alloys having increasing Ni concentrations (up to 2 wt%) were examined. The alloys were solution treated at 495 °C for 8 h and subsequently quenched into water at room temperature. Afterwards, the samples were overaged at 250 °C for 100 h. By adding 1 wt% Ni, the yield strength increased by approximately 70%. In contrast, it was observed in this work that the T6 heat-treated alloy has a significantly lower yield strength compared to the corresponding base alloy (approximately - 55%). This is probably linked to the different solutionising stages temperatures. As a matter of fact, the higher solutionising temperature applied in this work has probably led to an enhanced fragmentation and spheroidisation of Ni-rich intermetallic phases, which cannot thus form any rigid thermally stable 3D interconnected structure along with the eutectic Si phase. It should be interesting to study the same heat treatment for our alloys to focus on the change of the values of the yield strength and of the ultimate tensile stress. After that the mechanical results should be compared to Stadler's investigations.

About the maximum load (F_{\max}), as shown in the Figure 33, the value seems not to be affected by Ni additions in the as cast condition. The value of the maximum load decreases with an increase of the Ni content. The T6 condition shows the same trend.

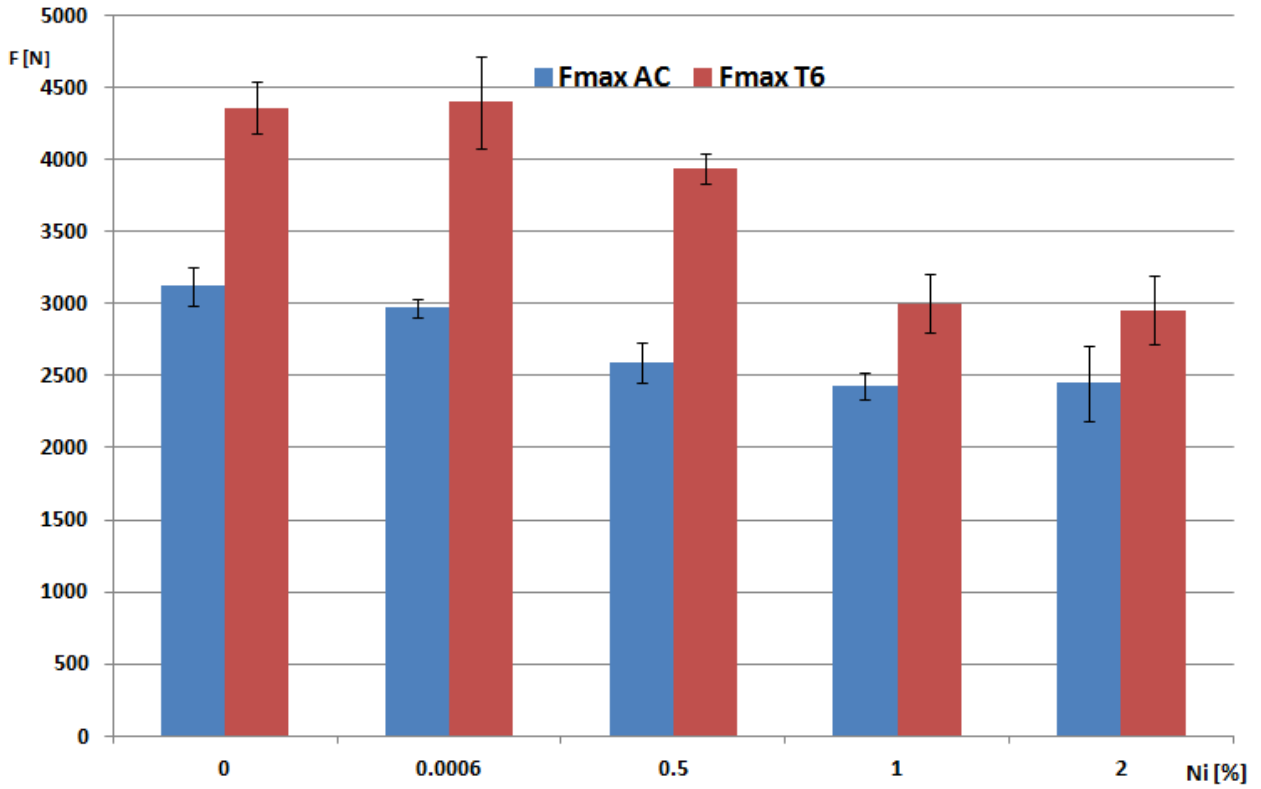


Figure 33 – The F_{max} in the As Cast and T6 condition

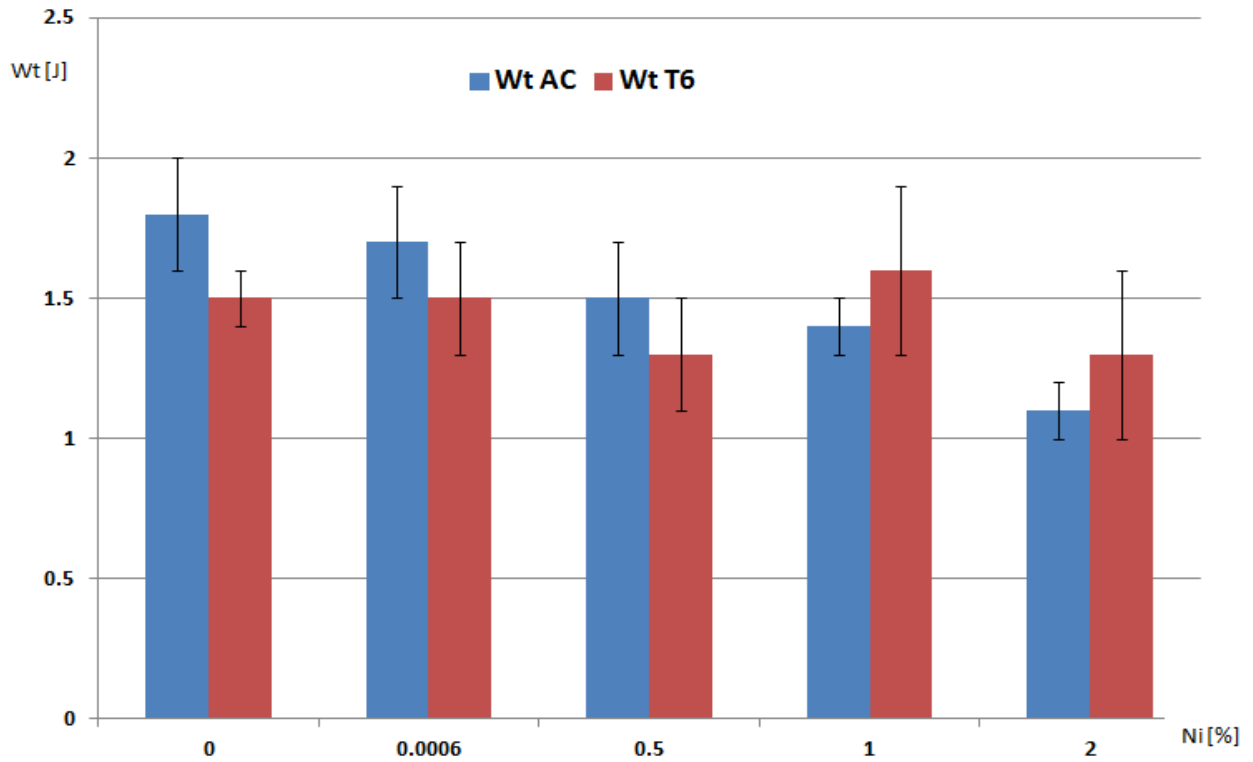


Figure 34 – The Wt in the As Cast and T6 condition

The increasing in Ni influences both the absorbed total energy (W_t) and the maximum load. As shown in Figure 33 and Figure 34, the increase in Ni allows the development of the component of the intermetallic phases. They are brittle phases and this determines lower values of the maximum load and the absorbed total energy.

The result is that both of the values decrease with the increasing of the Ni content.

Conclusions

The influence of Ni on the high temperature tensile properties and on the impact properties of a commercial purity unmodified A356 foundry alloy in both the as cast and T6 heat-treated conditions was studied in the present thesis. The influence of Ni on the high-temperature tensile properties and on the impact properties of a commercial purity unmodified A356 foundry alloy in the as-cast and T6 heat-treated conditions was studied in the present thesis.

As concern the high-temperature tensile tests, it was found that Ni contents higher than 0.5 wt% yield a significant reduction in both **R_{p0.2}** and **UTS** of the T6 heat-treated alloys. As a result, the mechanical properties become comparable with those of the corresponding as cast alloys. This suggests that the beneficial effect of T6 heat treatment is neutralised to some extent by the early fracture of the Ni-rich intermetallic phases. SEM investigations confirm the presence of **Ni-rich particles** on the fracture surfaces. Minor differences in the fracture path are observed between the as cast and the T6 heat-treated alloys.

As a result of the impact strength tests, total absorbed energy (W_t) and maximum load (F_{max}) seem not to be increased from the addition of 1 wt% Ni to the addition of 2 wt% Ni.

The increase in Ni allows the development of the component of the intermetallic phases. Both of the values decrease by increasing in Nickel

Moreover, both W_t and F_{max} decrease with respect to the reference as cast alloy (A356 – AC).

It has been observed that the addition of 2 wt% Ni condition seems to be not relevant, compared to the addition of 1 wt% Ni, for the high temperature tensile results and impact properties.

Acknowledgements

I would like to express my sincere gratitude to Prof. Mattia Merlin, who help me during the time that I spent in Trondheim. Thank you for the suggestions, thank you for help me weekly and thank you for the bureaucratic matters before and during my stay at the Norwegian University of Science and Technology (NTNU). Thank you also for the revisions during evenings and the week end. Thank you for your support.

Thank you also to Prof. Gian Luca Garagnani for your availability and your suggestion before my departure to Norway.

I would like to express my sincere gratitude to Prof. Marisa Di Sabatino Lundberg. Thank you for help me during my time in Trondheim, thank you for the availability and the suggestions. Thank you for the Christmas gift and thank you for your time. Thank you Prof. Yanjun Li for the suggestions about heat treatment and thank you also for your suggestions about the solidification curves.

I would like to express my gratitude to Dr. Arne Nordmark, Dr. Pål Skaret and Dr. Kurt Sandaunet for the casting processes, hot tensile tests and heat treatment respectively.

In the end I really want to thank you Ing. Daniele Casari. Working with you, was a pleasure: your talent, your way of speaking and your humanity impressed me every day. Thank you for your dedication, your comprehension and thank you for your generosity since the first day when I needed to find a pillow and you helped with the route. Thank you Daniele.

Thank you to my Norwegian friends that I knew in Moholt and thank you to Ntnui volleyball herrer team. All of you guys gave me something special that I appreciated. Thank you for your friendship.

Thank you to all my friends in Italy, the friends that I had since I was born, the friends that I knew in this years. I really appreciated since few years ago that happiness is only real when shared, so thank you for give me the opportunity to share my happiness with all of you.

Thank you also to “Squadraneri”; “Monsangeles”; “Gli amici di FedePo”; “Per pochi intimi”;”Liceo 5’I”.

Thank you to my friend Ennio, only you know how important was to arrive at this checkpoint; thank you for your loyalty, your dedication, your way of talking and thank you for all the time that we overtook a “mountain”. It seemed to be arduous but we didn’t feel the pain because we were together. Thank you for your friendship, bro!

Thank you to my family. The guidance, the patience that you gave in this years were unbelievable. Thank you to Riccardo, Francesco and Caterina. I really love you. That’s the reason that we argue sometimes.

The last and uttermost thanks goes to my mum. I felt really impressed by you since I was born. Your talent, patience, humanity impressed me since the first years of my life. You gave me bricks for built respect, books for teach me culture, you give smile for teach me love. Thank you for all the unwritten trainings and all the sentences.

Thank you for all the time that I felt down and you gave me a hand to pick up again by myself. That was one of the precious gift that you taught me. Thank you for being my mother, without you, this master would not have be possible, literally.

References

- [1] L. Bäckerüd, G. Chai, J. Tamminen, “Solidification Characteristic of Aluminium Alloys- vol 2: Foundry alloys”
- [2] L. Arnberg, L. Bäckerüd, G. Chai, “ Solidification Characteristics of Aluminum Alloys ” Vol III, 93- 95.
- [3] N.A. Belov, D.G. Eskin, A.A. Aksenov, “Casting alloys: applications for commercial aluminum alloys” Elsevier Science (2005).
- [4] J. Granfield, L. Sweet, C. Davidson, J. Mitchell, A. Beer, S. Zhu, X. Chen and M. Easton “An initial assessment of the effects of increased Ni and V in A356 and AA6066” Light Metal 2013, 2013, 39-45.
- [5] S. Zhu, J-Y. Yao, L. Swee, M. Easton, J. Taylor, P. Robiso, and N. Parson: “ Influence of Nickel and Vanadium impurities on microstructure of Aluminium alloys”, JOM 2013
- [6] Garcia, J.A. Hinojosa, C.R. Gonzalez, C.M. Gonzalez and Y. Houbaert: J. Mater. Process. Tech., 2003, vol. 143-144, pp. 306-310.
- [7] T. Ludwig P. L. Schaffer, L. Arnberg “ Influence of Some Trace Elements on Solidification Path and Microstructure of Al-Si Foundry Alloys” Metall. Mater. Trans. A, vol. 44A(2013), pp. 3783-3796.
- [8] D. Casari, Thomas H. Ludwig, M. Merlin, L. Arnberg, G. L. Garagnani “The effect of Ni and V trace elements on the mechanical properties of A356 aluminium foundry alloy in as-cast and T6 heat treated conditions” submitted to Materials Science and Engineering A
- [9] Z. Ashgar, G. Requena, F. Kubel, Material Sci. Eng. A 527 (2010) Materials Science and Engineering A 527 (2010) 5691–5698

[10] L.Heusler, F.J. Feikus, M.O. Otte, Afs Trans 109 (2001) AFS Transactions 01-050, pp.215-223.

[11] D. Casari, Thomas H. Ludwig, M. Merlin, L. Arnberg, and Gian Luca Garagnani
“Impact Behavior of A356 Foundry Alloys in the Presence of Trace Elements Ni and V” _ASM International DOI: 10.1007/s11665-014-1355-3 1059-9495/\$19.00

[12] F. Stadler “The effect of Ni on the high-temperature strength of Al-Si cast alloys.” Materials Science Forum Vol. 690 (2011) pp 274-277

[13] A.R. Farkoosh “Phase formation in as-solidified and heat-treated Al-Si-Cu- Mg-Ni alloys: Thermodynamic assessment and experimental investigation for alloy design” Journal of Alloys and Compounds 551 (2013) 596–606

